This article was downloaded by:
On: *28 January 2011*
Access details: *Access Details: Free Access*
Publisher *Taylor & Francis*
Informa Ltd Registered in England and Wales Registered Number: 1072954 Registered office: Mortimer House, 37-41 Mortimer Street, London W1T 3JH, UK

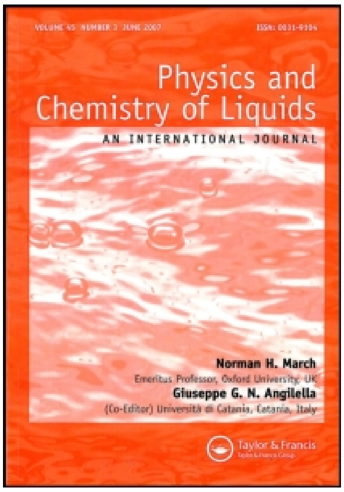

Physics and Chemistry of Liquids

Publication details, including instructions for authors and subscription information:
http://www.informaworld.com/smpp/title~content=t713646857

Electronic Correlation Functions in Liquid Metals

N. H. March[a]
[a] Oxford University, Oxford, England

To cite this Article March, N. H.(1999) 'Electronic Correlation Functions in Liquid Metals', Physics and Chemistry of Liquids, 37: 5, 479 — 492

To link to this Article: DOI: 10.1080/00319109908035932

URL: http://dx.doi.org/10.1080/00319109908035932

PLEASE SCROLL DOWN FOR ARTICLE

Full terms and conditions of use: http://www.informaworld.com/terms-and-conditions-of-access.pdf

This article may be used for research, teaching and private study purposes. Any substantial or systematic reproduction, re-distribution, re-selling, loan or sub-licensing, systematic supply or distribution in any form to anyone is expressly forbidden.

The publisher does not give any warranty express or implied or make any representation that the contents will be complete or accurate or up to date. The accuracy of any instructions, formulae and drug doses should be independently verified with primary sources. The publisher shall not be liable for any loss, actions, claims, proceedings, demand or costs or damages whatsoever or howsoever caused arising directly or indirectly in connection with or arising out of the use of this material.

Phys. Chem. Liq., 1999, Vol. 37, pp. 479–492
Reprints available directly from the publisher
Photocopying permitted by license only

Published by license under
the Gordon and Breach Science
Publishers imprint.
Printed in Malaysia.

Review Article

ELECTRONIC CORRELATION FUNCTIONS IN LIQUID METALS

N. H. MARCH*

Oxford University, Oxford, England

(Received 29 December 1997)

To determine experimentally the three pair correlation functions $g_{ii}(r)$, $g_{ie}(r)$ and $g_{ee}(r)$ in a pure liquid metal, i denoting ions and e electrons, requires three independent diffraction measurements. A brief review will be given in this difficult area, but progress is quite slow. One can make headway by confronting available experimental diffraction data with the results of computer experiments, and in particular on $g_{ie}(r)$. This will be illustrated with specific reference to recent computer simulations on liquid Mg and liquid Bi. For Mg, analytic modelling is also possible and this will be discussed.

Quite independently, computer experiments have recently appeared which describe the effects of isochoric heating on dense fluid hydrogen over a wide temperature range. This prompts again reference to analytic models, both caged atomic and molecular hydrogen being considered. Finally, though the electrical conductivity of the H plasma above has not yet been studied, a brief discussion of a possible mechanism of electronic transport in strongly coupled plasma will be presented.

Keywords: Two-component plasma; electron–ion correlation function; dense fluid hydrogen

1. INTRODUCTION

Substantially more than two decades ago, Egelstaff *et al.* [1] drew attention to the importance of extracting electronic correlation functions in liquid metals by combining X-ray, electron and neutron diffraction experiments. Then, for example, on liquid Mg, to be discussed at some length below, which can be considered as a two-

---

* Address for correspondence: 6, Northcroft Road, Egham, Surrey TW20 0DU, U.K.

component system (March and Tosi [2]) of ions Mg^{++} and electrons e^-, one could, at least in principle, extract the three partial structure factors $S_{nn}(q)$, $S_{nv}(q)$ and $S_{vv}(q)$, where n denotes nucleus and v is short for valence electrons. In early work (Watabe and Hasegawa [3], Chihara [4]), it was demonstrated that these three partial structure factors were related to the valence, say z, of the liquid metal by

$$S_{nv}(0) = z^{1/2} S_{nn}(0), \tag{1}$$

$$S_{vv}(0) = z S_{nn}(0), \tag{2}$$

while, from fluctuation theory, the nuclear structure factor $S_{nn}(0)$ at $q = 0$ is given by (see *e.g.*, Faber [5]):

$$S_{nn}(0) = n_i k_B T K_T, \tag{3}$$

n_i being the number of ions per unit volume, $k_B T$ the thermal energy and K_T the isothermal compressibility. These relations (1)–(3) will be important in some of the models to be discussed below (March and Tosi [6]).

In Section 2, the relation of the above three partial structure factors to X-ray scattering will be briefly summarized, following Egelstaff *et al.* [1]. However, it is important to note here that it has already been assumed in the above structural description that the electrons in a liquid metal such as Mg or Bi can be usefully classified into core and valence categories. In what follows, the core electrons will be assumed rigidly attached to the nuclei. Only the valence electrons therefore are described by the partial structure factors $S_{nv}(q)$ and $S_{vv}(q)$, and these two quantities will clearly enter the intensity of X-ray (and electron) diffraction from such liquid metals. However, the third partial structure factor, $S_{nn}(q)$, is directly accessible *via* neutron scattering. One recent neutron experiment which can be cited in the above context is on liquid K just above its freezing point (Johnson *et al.* [7]).

2. X-RAY SCATTERING FROM A LIQUID METAL

The X-ray scattering intensity $I_X(q)/N$ per atom is essentially the Fourier transform of the density–density correlation function

$\langle \rho(\mathbf{r})\,\rho(\mathbf{r}')\rangle$:

$$\frac{I_x(q)}{N} = \int \langle \rho(\mathbf{r})\rho(\mathbf{r}')\rangle \exp\,(i\mathbf{q}\cdot\mathbf{r}-\mathbf{r}')d\mathbf{r}\,d\mathbf{r}' \tag{4}$$

Effecting the core-valence separation discussed above by writing $\rho = \rho_c + \rho_v$, one can rewrite Eq. (4) in the form

$$\frac{I_x(q)}{N} = f_c^2(q)\ S_{nn}(q) + 2\tilde{F}\langle\rho_c(\mathbf{r})\rho_v(\mathbf{r}')\rangle + \tilde{F}\langle\rho_v(\mathbf{r})\rho_v(\mathbf{r}')\rangle \tag{5}$$

where $\tilde{F}$ denotes Fourier transform. But as mentioned the core electrons are assumed 'tied' to nuclei and hence one has

$$\frac{I_x(q)}{N} = f_c^2(q)\ S_{nn}(q) + 2f_c(q)\ S_{nv}(q) + \tilde{F}\langle\rho_v(\mathbf{r})\rho_v(\mathbf{r}')\rangle \tag{6}$$

In Eqs. (5) and (6), $f_c(q)$ denotes the scattering factor of the core, *i.e.*, of Mg^{++} or Bi^{5+} for these two liquid metals to be treated further below. A similar expression for electron scattering has been written down by Egelstaff *et al.* [1].

2.1. Diffraction and Computer Experiments Relating to Electron – Ion Correlations

Direct experimental extraction of $S_{nv}(q)$ from diffraction measurements has so far proved difficult and progress has been therefore slow. The interested reader may refer to the review by Tamaki [8]; see however Steeb *et al.* [9]. We shall refer to such efforts again below, when we report, and analyze further, computer studies of electron – ion correlations.

We note, however, that for real progress using diffraction experiments it is essential to have high accuracy measurements using neutrons, X-rays and electrons on the same liquid metal under similar thermodynamic conditions. A full comparison of X-ray and neutron measurements on liquid K near freezing is presented by Johnson *et al.* [7] but unfortunately, to our knowledge, electron diffraction data is not available on this liquid metal near freezing at the time of writing.

3. COMPUTER SIMULATION ON ELECTRON-ION INTERACTION IN LIQUID MG

Though experimental diffraction studies to extract the electron-ion partial structure factor $S_{n\nu}(q)$ remain very difficult quantitatively, a major step forward in this general area has been taken by de Wijs *et al.* [10]. These workers follow Car and Parrinello [11] in combining molecular dynamics and density functional theory. They have, essentially, studied the valence electron density in liquid Mg (and also in liquid Bi, to be discussed also briefly below).

First of all, their calculated nuclear-nuclear structure factor $S_{nn}(q)$ can be compared with the measured $S_{nn}(q)$ for liquid Mg under comparable thermodynamic conditions. Experiment and theory are in good agreement.

3.1. Analytic Modelling to Expose Origin of Main Features in Electron-Ion Structure Factor $S_{n\nu}(q)$

On inspection of the computer data of de Wijs *et al.* [10], one sees that there is antiphase behaviour between $S_{nn}(q)$ and $S_{n\nu}(q)$ at the principal peak of the structure factor. In the modelling of March and Tosi [6], referred to as MT, it becomes quite clear what is the origin of this antiphase characteristic. Thus, MT give a formula for $S_{n\nu}(q)$ which they have used to analytically model the ratio $S_{n\nu}(q)/S_{nn}(q)$. The study of this ratio is motivated by Eq. (1), which relates the long wavelength limit of this quantity to the valence z(2 for liquid Mg near its freezing point). MT have then modelled $S_{n\nu}(q)/S_{nn}(q)$ using the simplest possible input. This is (i) a pseudopotential $v(k)$ representing the electron-ion interaction in Mg and (ii) a dielectric function $\varepsilon(q)$ accounting for metallic screening. No attempt was made to use refined choices. MT employ an Ashcroft pseudopotential for $v(q)$ characterized by a valence $z = 2$ and an Ashcroft radius already available in the literature. These workers simply used the Thomas-Fermi dielectric function

$$\varepsilon_{\mathrm{TF}}(q) = \frac{q^2 + q_{\mathrm{TF}}^2}{q^2} \tag{7}$$

where the Thomas-Fermi inverse screening length q_{TF} is determined from the Fermi wave number k_f by

$$q_{\mathrm{TF}}^2 = \frac{4k_f}{\pi a_0} : a_0 = \frac{\hbar^2}{me^2}. \tag{8}$$

The main features of the computer data of de Wijs *et al.*, are then to be understood on the basis of the MT model summarised below. Their result employed is

$$\frac{S_{nv}(q)}{S_{nn}(q)} = \frac{z^{1/2}v(q)}{(4\pi e^2/q^2)}\left[\frac{1}{\varepsilon(q)} - 1\right] \tag{9}$$

The Ashcroft empty core form of $v(q)$ is

$$v(q) = \frac{-4\pi ze^2}{q^2}\cos(qR_c) \tag{10}$$

The literature value of $R_c = 1.39a_0$ was adopted for Mg, with $z = 2$ near freezing. The antiphase behaviour of $S_{nv}(q)$ with respect to the nuclear structure factor $S_{nn}(q)$ is due to the fact that the node in the pseudopotential occurs at a q value inside that characterizing the first peak in $S(q)$. Though no attempt was made to adjust the modelling to be fully quantitative, in fact all the essential features $S_{nv}(q)$ are already clear. The ratio $S_{nv}(q)/S_{nn}(q)$ according to the modelling of MT is displayed in Figure 1. We want to stress that in liquid Mg, the use of weak electron–ion interaction is valid.

To add a few comments relating to the comparison of the modelling shown in Figure 1 with the computer investigations on Mg, the node is at 2.1 Å^{-1} in the computer results: nearly predicted correctly by the MT model. The deepest value of the ratio shown in -0.13 whereas from the computer study of de Wijs *et al.*, it is -0.08.

MT also plot the same ratio, but now directly from the computer results for liquid Bi, and their results are shown in Figure 2. The extrapolated ratio from the data of de Wijs *et al.* [10] passes satisfactorily through the long wavelength limit $z^{1/2}$ with $z = 5$ for liquid Bi, as it must from the theoretical result (1) representing perfect screening, or equivalently the fact that long-range electric fields cannot exist in a metallic medium.

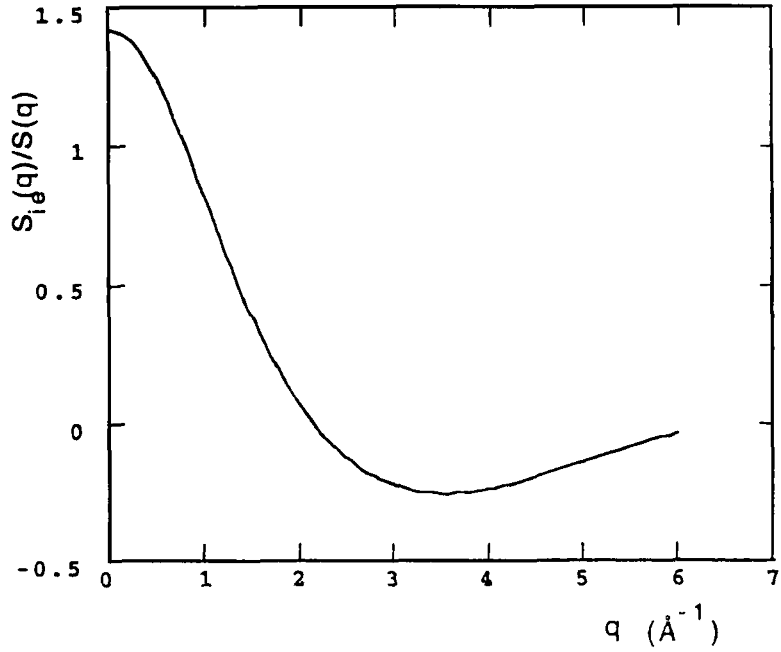

FIGURE 1 Ratio of electron–ion to nuclear–nuclear partial structure factors for liquid Mg near freezing, following March and Tosi [6]. Note that ratio at $q = 0$ is $z^{1/2}$, with valence $z = 2$ for Mg. Curve shown is constructed from Eq. (9) with $v(q)$, the electron–ion pseudopotential as in Eq. (10), with the Ashcroft radius $R_c = 1.39a_0 : a_0 = \hbar^2/me^2$. The Thomas-Fermi dielectric function in Eq. (7) was used in constructing curve in Figure. All the main features of the computer studies of de Wijs *et al.* [10] are apparent in the modelling displayed in this figure, with no adjustable parameters, as the literature value of R_c was adopted.

To sum up briefly, the assumption of weak electron–ion interaction, plus the simplest possible choices of electron–ion pseudopotential $v(q)$ in Eq. (10) and dielectric function $\varepsilon(q)$ in Eq. (7) satisfactorily account for the main features of the computer data of de Wijs *et al.* [10] on liquid Mg near freezing, as demonstrated in the work of March and Tosi [6]. However, such a simple treatment cannot be expected to work for liquid Bi, for though Hall effect measurements show that $z = 5$, crystalline Bi is a semimetal and this testifies to the fact that there the electron–ion interaction cannot be assumed weak.

de Wijs *et al.* [10] in their important study make contact with the diffraction data of Tamaki *et al.* [12]. Especially for Bi, it is a challenge

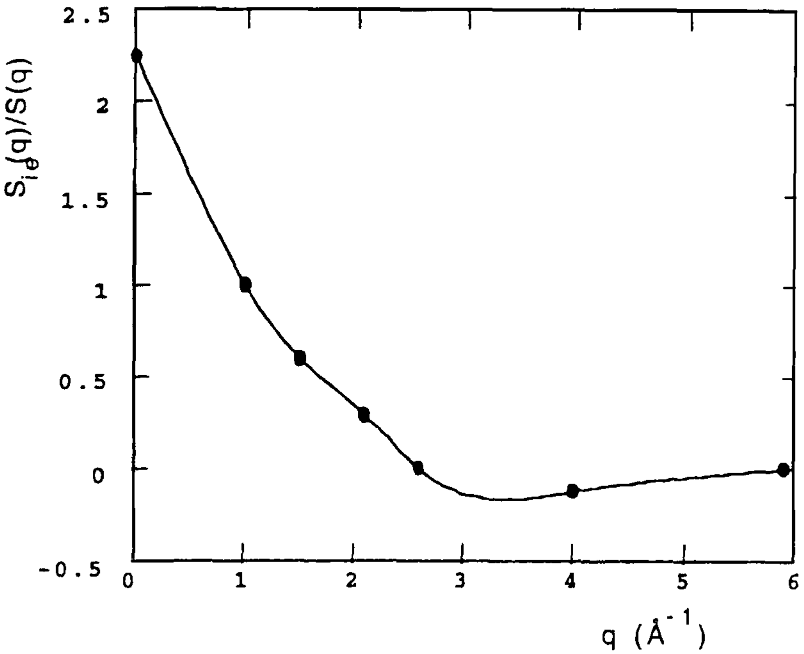

FIGURE 2 Similar to Figure 1 except that no model was invoked, the ratio of structure factors shown for liquid Bi being constructed by March and Tosi [6] directly from the computer data of de Wijs *et al.* [10]. There is no difficulty in extrapolating the computer results to pass through the theoretical limit $z^{1/2}$, given in Eq. (1) with $z = 5$.

for the experimentalist to see whether a quantitative account of Figure 2 can be obtained directly from experiment.

We conclude this section with a few brief comments on electron–electron correlations. It is tempting, from Eq. (6) for the X-ray intensity, to try to exploit the fact that the node in $S_{nv}(q)$ for Bi at around 2.1 Å^{-1} should 'expose' the electron–electron term at this value of q. Again, it is a challenge to experimentalists to see whether there one can establish with certainty a difference between $I_x(q)/N$ and $f_c^2(q)\ S_{nn}(q)$, as required by Eq. (6). This is presumably going to require considerable accuracy not only in the neutron and X-ray experiments needed for $S_{nn}(q)$ and $I_x(q)$ respectively but also in the quantum chemical calculation of the 'core' scattering factors $f_c(q)$. It remains of considerable interest to see if electron–electron correlations can be exposed by such diffraction studies. Refinement of electron diffraction measurements (Brah *et al.* [13, 14]) seems also a matter of high priority in this area.

We turn next to discuss electronic properties in dense fluid hydrogen [15].

4. COMPUTER SIMULATION OF DENSE FLUID HYDROGEN UNDER ISOCHORIC HEATING

To briefly introduce this section on dense fluid hydrogen, we begin by writing the internal energy E, which involves both electronic kinetic energy K and the kinetic energy of the ions K_{ion}. The result is (see *e.g.*, March and Tosi [16]):

$$E = K_{\text{ion}} + K + \frac{1}{2n_i}\int d\mathbf{r}\left[n_e^2 g_{ee}(r)\,\frac{e^2}{r} + n_i^2 g_{ii}(r)\,v_{ii}(r) + 2n_i n_e g_{ie}(r)\,\tilde{v}(r)\right] \tag{11}$$

In Eq. (11), the three partial radial distributions are evidently involved. The bare ion–ion potential is denoted by $v_{ii}(r)$, while $\tilde{v}(r)$ is the electron–ion interaction potential.

The computer simulation experiment of Magro *et al.* [15] has yielded the electronic kinetic energy K over a wide range of temperature T, for three densities. With the usual plasma parameter r_s measured in units of the Bohr radius a_0, related to the mean electron density ρ by

$$\rho = \frac{3}{4\pi r_s^3 a_0^3} \tag{12}$$

Figure 3 of the article by Magro *et al.* plots K *vs* T for $r_s = 1.86$, 2.0 and 2.2.

In the low temperature regime, one has molecular H_2 fluid whereas in the very hot assembly one has an atomic fluid. March and Tosi [17] attempted to gain insight, *via* admittedly somewhat crude models, into the variation of K with r_s (at constant temperature T say) in both the atomic and the molecular fluid regions.

4.1. H Atom in Cage

March and Tosi [17], in the high T regime of the computer results of Magro *et al.*, have analyzed the ground-state electronic kinetic energy K by using the model of a H atom enclosed by a spherical boundary of radius a with the proton at the centre. The wave function of the electron is put to zero at a. Using 2*s* and 3*s* wavefunctions ($\psi_{no}(r)$), each truncated at their innermost node, March and Tosi have plotted $K(a)$.

Subsequently, the writer has noted the 'boundary perturbation theory' developed by Barton *et al.* [18]. This allows one to calculate analytically the change $\Delta K = K(a) - K(\infty)$, where $K(\infty)$ is the usual H atom result

$$K(\infty) = -E(\infty) = \frac{e^2}{2a_0} \tag{13}$$

as follows from the usual hydrogenic 1*s* level plus the virial theorem.

Writing

$$u(r) = r\psi_{10}(r, a = \infty) \tag{14}$$

Barton *et al.* show first that one can write the energy change $\Delta E(a)$ entirely in terms of quadratures on the free space ($a = \infty$) quantity $u(r)$. Their result is given by

$$\frac{2m}{\hbar^2}\Delta E(a)\int_0^a \frac{dr_1}{u^2(r_1)}\int_0^{r_1} dr_2\, u^2(r_2) = 1. \tag{15}$$

Inserting $\psi_{10}(r)$ into Eqs. (14) and (15), one finds

$$\frac{\Delta E(a)}{|E(\infty)|} = 8\left(\frac{a}{a_0}\right)^2 \exp\left(\frac{-2a}{a_0}\right)\left[1 + O\left(\frac{a_0}{a}\right)\right]. \tag{16}$$

Now one invokes the virial theorem in the form

$$\Delta K + \Delta E = -\frac{a\,d\Delta E}{da} \tag{17}$$

which relates $\Delta K(a)$ and $\Delta E(a)$. Combining therefore Eqs. (16) and (17) yields the desired result

$$\Delta K(a) = 16|E(\infty)|\left(\frac{a}{a_0}\right)^3 \exp\left(\frac{-2a}{a_0}\right)\left[1 + O\left(\frac{a_0}{a}\right)\right] \tag{18}$$

This form (18) at small (a_0/a) fits well between the exact results of March and Tosi [17] from the 2*s* and 3*s* truncated wave functions and the value zero at $a = \infty$. The truncated 2*s* wave function at its node $2a_0$ corresponds to the Magro calculation for $r_s = 2$. The cage model H gives $K(2a_0) = 2.8$ Ryd which is substantially larger than the computer value of 1.6 Ryd. Similarly for $r_s = 1.86a_0$, the model gives ~ 0.2 Ryd, while the computer value is nearer 0.05 Ryd. The cage model therefore substantially overemphasizes the effect of compression on fluid hydrogen. This is confirmed by March and Tosi [17] by results obtained by softening the (infinite) barrier of the cage model.

4.2. H_2 Molecule With Electron–Electron Interactions, in Appropriate Cage

Using the careful study for LeSar and Herschbach [19], including electron–electron correlations, March and Tosi have repeated the calculations of *K vs* volume for the H_2 molecule in a spheroidal cage. Again, the gist of the variation found in the computer experiment is given by the model, but again the effect of compression is overemphasized by the infinite barrier model. As well as the kinetic energy, the internuclear distance of H_2 as a function of r_s is given in semiquantitative form by the cage model.

We now turn to the question of electrical conductivity, which was not reported on by Magro *et al.* [15] for dense fluid hydrogen in the final section.

5. MODEL OF ELECTRICAL CONDUCTIVITY OF STRONGLY COUPLED PLASMA

The idea presented in an earlier study (March and Tosi [20]) of the electrical conductivity of Cu plasma was to start from the Nernst-Einstein relation between mobility μ and electronic diffusion coefficient, *D*, namely

$$\mu = \frac{D}{k_B T} \tag{19}$$

where k_BT is the thermal energy associated with temperature T. Writing the conductivity in terms of the electron density n_e through

$$\sigma = n_e e^2 \mu \tag{20}$$

one finds immediately using Eq. (19)

$$\sigma = \frac{n_e e^2 D}{k_B T} \tag{21}$$

Rearranging Eq. (21) so that $Dn_e^{2/3} \propto D/(\text{length})^2$ appears, as in the previous work, (March and Tosi [20]) Eq. (21) becomes

$$\sigma n_e^{1/3} T = (Dn_e^{2/3})\left(\frac{e^2}{k_B}\right) \tag{22}$$

For monovalent Cu, $Dn_e^{2/3} = Dn_i^{2/3}$ turned out to be independent of the thermodynamic state in the strongly coupled plasma regime (March and Tosi [20], DeSilva and Kunze [21]).

This has therefore motivated a plot for W plasma of the quantity Y defined by

$$Y = \sigma n_i^{-1/3} T \tag{23}$$

as a function of temperature T. Note that Y differs from the left-hand side of Eq. (22) by a factor proportional to the cube root of the effective valence Z.

While σ and n_i are well specified in the paper of Kloss *et al.* [22] on tungsten plasma there is some question as the choice of data for the temperature. Thus, in the upper part (a) of their Figure 5, they plot measured temperature of the wire *vs* n_i for a wire explosion with lowest and highest energy input. Data has been used from both these curves. The product $Y = \sigma n_i^{-1/3} T$ turns out in both cases, even though there is considerable scatter at least partly coming from reading off of the data, to decrease substantially with increasing temperature T. The above argument, based on Eqs. (19)–(23), would interpret this decrease as reflecting the variation of $Z^{1/3}$ with temperature.

Under 'normal' conditions, Slater [23], for example, records the outer electronic configuration of the W atom as sd^5, suggesting, as noted also by Kloss *et al.*, that near the melting point $Z = 6$. Likalter in a private communication to Kloss *et al.*, has proposed $Z \approx 3$ at the critical point, and for the maximal observed expansion in their work Kloss *et al.*, propose $Z \approx 1$. These values are not inconsistent with the curves given in Figures 1 and 2 of March and Tosi [24] bearing in mind the substantial scatter among the points plotted.

To sum up, the earlier interpretation offered from the results on Cu plasma obtained in the conductivity measurements of DeSilva and Kunze [21] has been shown by March and Tosi [24] to permit the extraction of the effective valence Z as a function of temperature for W plasma from conductivity measurements. The results are quite compatible with the proposals made by Kloss *et al.* [22].

Subsequently, and in a somewhat different context, the same model as above has been used to interpret conductivity data on double-walled C nanotubes (March, Alonso and Rubio [25]).

6. SUMMARY AND FUTURE DIRECTIONS

The advent of computer studies such as those of de Wijs *et al.* [10] on liquid Mg and Bi near freezing and Magro *et al.* [15] on isochoric heating of dense fluid H over a vast range of temperature has greatly aided progress in the two-component theory of liquid metals. While Mg and Bi in the liquid state studied by de Wijs *et al.*, are undoubtedly good metals, it remains to be seen what is the electrical conductivity behaviour of dense fluid hydrogen over the range of thermodynamic states studied by Magro *et al.* [15].

However, it is highly relevant in the above context to record that shock wave measurements of Weir *et al.* [26] on liquid H and liquid D have unambiguously established that an insulator-metal transition occurs at high temperatures and at a pressure ~ 1.5 megabar. The point we need to stress here is that in the metallic phase observed to date there is coexistence with chemical bonding. Though the actual electrical resistivity is comparable with that observed in the heavy alkali liquid metal Rb (see Weir *et al.* [26]), the behaviour of liquid H and D seems more akin to that found in solid iodine, though in a much more accessible thermodynamic range in this latter material. Here, beyond question, the experimental electrical resistivity measurements of Drickamer [27] show a metallic phase at ~ 150 kbar, while at the same time diffraction experiments clearly reveal a 'molecular' metal with a well defined I_2 bond length. These two observations have been reconciled in the study of Siringo *et al.* ([28]; see also [29]). The mechanism of the metal-insulator transition here is energy band overlap, the gap in the insulating/semiconducting phase being gradually closed by application of laboratory pressures.

However, it must be emphasized that in the experiments of Weir *et al.* [26] the high temperatures are playing an important role in the insulator-metal transition in dense fluids H and D. These authors, in fact, conjecture that in the cold solids the applied pressure will probably need to be increased to the order of 3.5 megabar.

The work on H and D certainly needs following with both experiment and theory, particularly on electrical conductivity. The Nernst-Einstein approach of Section 5 would suggest electronic hopping as a possible mechanism here. One important consequence of that would be that the high-frequency conductivity $\sigma(\omega)$ should have power law behaviour, of the form σ proportional to ω^n with the exponent $n \sim 0.8$. This is to be contrasted with Drude-Zener type behaviour of the form $\sigma(\omega) = \sigma(0)/[1 + \omega^2\tau^2]$, with τ the relaxation time. For $\omega\tau \gg 1$ this leads to $\sigma(\omega) \alpha \omega^{-2}$.

To return finally to the matters raised in the Introduction, systematic work on one specific liquid metal is much needed. Since accurate X-ray and neutron experiments now exist on liquid K near freezing, this seems an obvious liquid metal on which to study electron diffraction. In parallel, it would be of interest if the computer simulation study paralleling those on liquid Mg and Bi could also be carried out on liquid K near freezing.

Acknowledgement

This article could not possibly have come to fruition without the great help of Professor Mario Tosi. It is a pleasure to acknowledge that the recent work reported was carried out during the tenure of visiting appointments in his group at the Scuola Normale Superiore in Pisa. Thanks are also due to Professor Renato Pucci and his colleagues at the University of Catania for invaluable discussions on the high-pressure behaviour of condensed iodine and condensed hydrogen.

Partial financial support for the work on liquid metals is acknowledged from the EC Network on 'High energy density matter', coordinated by Professor J. M. Martinez-Val (Madrid). Finally the writer is indebted to Professor Gabor Kalman for inviting him to deliver a Plenary Lecture at the Boston (1997) Conference on 'Strongly Coupled Plasma'. The present review resulted from that lecture.

References

[1] Egelstaff, P. A., March, N. H. and McGill, N. C. (1974). *Can. J. Phys.*, **52**, 1651.
[2] March, N. H. and Tosi, M. P. (1973). *Ann. Phys.* (NY) **81**, 414.
[3] Watabe, M. and Hasegawa, M. (1973). 2^{nd} *Int. Conf. Liquid Metals* (Taylor and Francis), p. 133.
[4] Chihara, J., Ref. 3, p. 137.
[5] Faber, T. E. (1972). Theory of Liquid Metals (Cambridge University Press, UK).
[6] March, N. H. and Tosi, M. P. (1998). Laser and particle beams, **16**, 71.
[7] Johnson, M. W., March, N. H., Perrot, F. and Ray, A. K. (1994). *Phil. Mag.*, **B69**, 965.
[8] Tamaki, S. (1987). *Can. J. Phys.*, **65**, 286.
[9] Steeb, S., Knoll, W. and Lamparter, P. Z. (1983). *Naturforsch.*, **38a**, 395.
[10] de Wijs, G. A., Pastore, G., Selloni, A. and van der Lugt, W. (1995). *Phys. Rev. Lett.*, **75**, 4480.
[11] Car, R. and Parrinello, M. (1985). *Phys. Rev. Lett.*, **55**, 2471.
[12] Tamaki, S., Takeda, S. and Waseda, Y. (1994). *J. Phys. Soc. Japan*, **63**, 1794.
[13] Brah, A. S., Virdhee, L., Unvala, B. and March, N. H. (1979). Inst. of Phys. Proc. (UK).
[14] Brah, A. S., Virdhee, L. and March, N. H. (1980). *Phil. Mag.*, **42**, 511.
[15] Magro, W. R., Ceperley, D. M., PieRLeoni, C. and Bernu, B. (1996). *Phys. Rev. Lett.*, **76**, 1240.
[16] March, N. H. and Tosi, M. P. (1984). Coulomb Liquids (Academic: New York).
[17] March, N. H. and Tosi, M. P. (1996). *Nuovo Cimento*, **18D**, 1061.
[18] Barton, G., Bray, A. J. and McKane, A. J. (1990). *Am. J. Phys.*, **58**, 751.
[19] LeSar, R. and Herschbach, D. R. (1981). *J. Phys. Chem.*, **85**, 2798.
[20] March, N. H. and Tosi, M. P. (1995). *Phys. Chem. Liquids*, **29**, 273.
[21] DeSilva, A. W. and Kunze, H.-J. (1994). *Phys. Rev.*, **E49**, 4448.
[22] Kloss, A., Motzke, T., Grossjohann, R. and Hess, H. (1996). *Phys. Rev.*, **E54**, 5851.
[23] Slater, J. C. (1960). Quantum theory of atomic structure, Vol. I (McGraw-Hill, New York), p. 194.
[24] March, N. H. and Tosi, M. P. (1997). *Phys. Chem. Liquids*, in press.
[25] March, N. H., Alonso, J. A. and Rubio, A. (1997). *Phys. Stat. Solidi*, in press.
[26] Weir, S. T., Mitchell, A. C. and Nellis, W. J. (1996). *Phys. Rev. Lett.*, **76**, 1860.
[27] Drickamer, H. G. (1965). *Solid State Physics*, **17**, 1.
[28] Siringo, F., Pucci, R. and March, N. H. (1989). *High Pressure Research*, **8**, 1.
[29] March, N. H. (1992). *J. Math. Chem.*, **4**, 271.